Inducible expression of 15-lipoxygenase-2 and 8-lipoxygenase inhibits cell growth via common signaling pathways

Dorothea Schweiger, Gerhard Fürstenberger, and Peter Krieg[1]

Division of Eicosanoids and Tumor Development, German Cancer Research Center, D-69120 Heidelberg, Germany

Abstract **Human 15-lipoxygenase (LOX)-2 and mouse 8-LOX represent orthologous members of the LOX family but display different positional specificities and tissue distribution. To study the functional role of 15-LOX-2 and 8-LOX in keratinocytes, an inducible Tet-On gene expression system was established in the premalignant mouse keratinocyte cell line 308. Doxycycline (dox)-induced expression of enzymatically active 15-LOX-2 and 8-LOX led to an inhibition of cell growth that was associated with an inhibition of DNA synthesis, as shown by a 15–46% reduction of 5-bromo-2-deoxy-uridine (BrdU) incorporation. The inhibitory effects were increased in the presence of exogenous arachidonic acid. In contrast, addition of linoleic acid or the LOX inhibitor baicalein reversed the growth-inhibitory effects. Treatment of the cells with 15-hydroxyeicosatetraenoic acid (HETE) or 8-HETE resulted in a similar inhibition of BrdU incorporation, whereas 13-hydroxyoctadecadienoic acid (HODE) and 9-HODE, in contrast, had no effects. Dox-induced keratinocytes showed increased levels of reactive oxygen species (ROS). The antioxidant *N*-acetyl-L-cysteine and a specific inhibitor of p38 mitogen-activated protein kinase, but not of extracellular signal-regulated kinase 1/2 or c-Jun N-terminal kinase/stress-activated kinases, completely abolished the LOX-induced growth inhibition, indicating a critical role of ROS and p38. Our data suggest that 15-LOX-2 and 8-LOX, although displaying different positional specificity, may use common signaling pathways to induce growth inhibition in premalignant epithelial cells.—** Schweiger, D., G. Fürstenberger, and P. Krieg. **Inducible expression of 15-lipoxygenase-2 and 8-lipoxygenase inhibits cell growth via common signaling pathways. *J. Lipid Res.* 2007.** 48: **553–564.**

Supplementary key words keratinocyte • reactive oxygen species • antioxidant • mitogen-activated protein kinases

Lipoxygenases (LOXs) are a family of dioxygenases that insert one molecule of oxygen in a regioselective and stereoselective manner into specific positions of PUFAs such as arachidonic acid (AA) and linoleic acid (LA) to form hydroperoxyeicosatetraenoic acids (HPETEs) and hydroperoxyoctadecadienoic acids (HPODEs), respectively. Upon reduction, the corresponding hydroxyl derivatives hydroxyeicosatetraenoic acid (HETE) and hydroxyoctadecadienoic acid (HODE) as well as leukotrienes, hepoxilins, and lipoxins are produced (1). These oxidized metabolites are known to be critically involved in the regulation of many biological processes, and aberrant oxidative metabolism of PUFAs has been implicated in the pathogenesis of many human diseases, including atherosclerosis, rheumatoid arthritis, Alzheimer's dementia, and cancer (2). LOX products act as signaling mediators via the activation of G protein-coupled cell surface receptors in an autocrine or paracrine manner and as activating ligands of peroxisome proliferator-activated receptors (PPARs) via an intracrine mechanism. In addition, LOX-catalyzed metabolism is a rich source of reactive oxygen species (ROS), which are formed as side products of the hydroperoxidation of PUFAs (1, 3).

In mammalian tissues, LOXs enzymes are classified according to the position of oxygen insertion into AA as 5-, 8-, 12-, and 15-LOX. Four different 12-LOX isoenzymes have been characterized: the platelet-type, leukocyte-type, and epidermal 12S-LOX, and 12R-LOX. Furthermore, there are two 15-LOX enzymes, 15-LOX-1 and 15-LOX-2 (4). Finally, epidermal LOX-3 has been identified as a rather unusual member of the LOX family by exhibiting hydroperoxide isomerase rather than dioxygenase activity (5, 6). Based on their phylogenetic relationship, these mammalian LOX isoforms can be subdivided into four groups: the

Manuscript received 21 December 2005 and in revised form 17 July 2006 and in re-revised form 8 December 2006.

Published, JLR Papers in Press, December 11, 2006.
DOI 10.1194/jlr.M600311-JLR200

Abbreviations: AA, arachidonic acid; dox, doxycycline; BrdU, 5-bromo-2-deoxy-uridine; DCF, 2′,7′-dichlorofluorescein diacetate; ERK, extracellular signal-regulated kinase; HETE, hydroxyeicosatetraenoic acid; HODE, hydroxyoctadecadienoic acid; HPETE, hydroperoxyeicosatetraenoic acid; HPODE, hydroperoxyoctadecadienoic acid; JNK, c-Jun N-terminal kinase; LA, linoleic acid; LOX, lipoxygenase; MAPK, mitogen-activated protein kinase; NAC, *N*-acetyl-L-cysteine; PPAR, peroxisome proliferator-activated receptor; ROS, reactive oxygen species.

[1] To whom correspondence should be addressed.
e-mail: p.krieg@dkfz.de

5-LOX, the platelet-type 12-LOX, the 15/12-LOX, including the mouse leukocyte-type 12-LOX and human 15-LOX-1, and the recently discovered group of epidermis-type LOX (7). The latter type comprises the mouse and human 12R-LOX, the epidermal LOX-3, the mouse 8-LOX, and the human 15-LOX-2. The genes of the epidermis-type LOX are closely related and are located within a cluster at the central region of mouse chromosome 11. The genomic organization of the corresponding human gene cluster is highly conserved as a syntenic group at human chromosome 17p13.1 (8). Based on the high sequence identity and the conserved structure and chromosomal localization of the corresponding gene, 15-LOX-2 is regarded as the human ortholog of mouse 8-LOX. In fact, having 78% identity in amino acid composition, mouse 8-LOX and human 15-LOX-2 exhibit the highest sequence identity compared with all other mammalian LOXs (9–12). Moreover, it is intriguing that the exchange of only two amino acids, tyrosine 603 and histidine 604 of 8-LOX by the corresponding amino acids of 15-LOX-2 (i.e., asparagine and valine) converts the positional specificity from 8 to 15 and vice versa (13).

The fact that the human ortholog of the mouse 8-LOX encodes a LOX with different positional specificity (i.e., 15-LOX) is unique among all mammalian LOXs. Both enzymes are expressed in the skin of mice and humans but in different compartments of the epithelium. The expression of 15-LOX-2 is restricted to basal keratinocytes, whereas 8-LOX was found to be expressed in suprabasal keratinocytes (14, 15). 8-LOX preferentially metabolizes AA to 8-HPETE compared with LA, yielding 9-HPODE (16, 17). 15-LOX-2, on the other hand, was found to accept both AA and LA as substrates to generate 15-HPETE and 13-HPODE (18). To determine the function of the two orthologous LOXs in keratinocytes, we established an inducible expression system for 8-LOX and 15-LOX-2 in the mouse keratinocyte line 308.

MATERIALS AND METHODS

Materials

Cell culture media and supplements were purchased from Biochrom AG (Berlin, Germany). Culture dishes, flasks, and Nunc Lab-Tek eight-well glass object slides were from Renner GmbH (Dannstadt, Germany). Doxycycline (dox), *N*-acetyl-L-cysteine (NAC), and Hoechst dye 33258 were obtained from Sigma-Aldrich (Taufkirchen, Germany), and baicalein monohydrate was from Cayman Chemical (Ann Arbor, MI). 5*Z*,8*Z*,11*Z*,14*Z*-eicosatetraenoic acid (AA) and 9*Z*,12*Z*-octadecadienoic acid (LA) were from Sigma (München, Germany). 8(*S*)- and 8(*R*)-hydroxyeicosa-5(*Z*),9(*E*),11(*Z*),14(*Z*)-tetraenoic acid [8(*S*)-HETE and 8(*R*)-HETE], 15(*S*)- and 15(*R*)-hydroxyeicosa-5(*Z*),8(*Z*),11(*Z*),13(*E*)-tetraenoic acid [15(*S*)-HETE and 15(*R*)-HETE], 9(*S*)- and 9(*R*)-hydroxyoctadeca-10(*E*),12(*Z*)-dienoic acid [9(*S*)-HODE and 9(*R*)-HODE], and 13(*S*)- and 13(*R*)-hydroxyoctadeca-9(*Z*),11(*E*)-dienoic [13(*S*)-HODE and 13(*R*)-HODE] were from Reatec (Weiterstadt, Germany). Hygromycin B for cell culture was from Invitrogen GmbH (Karlsruhe, Germany). All other chemicals and solvents were of analytical grade.

Rabbit polyclonal anti-peptide antibodies were raised against a peptide corresponding to amino acids 56–83 of mouse 8-LOX. The 8-LOX antibody specifically recognizes recombinant mouse 8-LOX and does not show cross-reactivity with any other LOX isoenzyme (P. Krieg, unpublished data). Other primary antibodies used in this study include polyclonal rabbit anti-human 15-LOX-2 (Cayman Chemical), polyclonal goat anti-human β-actin (Santa Cruz Biotechnologies, Heidelberg, Germany), and monoclonal anti-mouse 5-bromo-2-deoxy-uridine (BrdU; Progen, Heidelberg, Germany). Secondary antibodies were goat anti-rabbit IgG-horseradish peroxidase-conjugated (Dianova, Hamburg, Germany), donkey anti-goat IgG-horseradish peroxidase-conjugated (Santa Cruz Biotechnologies), and Cy3-conjugated donkey anti-mouse IgG (Jackson ImmunoResearch Laboratories, Cambridgeshire, UK) antiserum.

Cell culture

Mouse keratinocyte line 308 was obtained from S. H. Yuspa (19). Cells were cultured in 4× MEM with a 4-fold concentration of amino acids and vitamins supplemented with 10% fetal bovine serum plus 100 U/ml penicillin and 0.1 mg/ml streptomycin (culture medium) at 34°C in a humidified atmosphere under 95% air and 5% CO_2. Tet-On experiments were done in 10% Tet system-approved fetal calf serum (BD Biosciences, Palo Alto, CA). The packaging cell line Phoenix-Eco was cultured in DMEM supplemented with 10% fetal bovine serum plus 100 U/ml penicillin, 0.1 mg/ml streptomycin, and 1 mM sodium pyruvate at 37°C in a humidified atmosphere with 5% CO_2. Cells were passaged every 3–4 days in fresh medium after release with trypsin-EDTA solution.

Construction of pRevTRE/LOX expression constructs

15-LOX-2 cDNA was isolated by a nested RT-PCR procedure as described previously (8) using a 3′-rapid amplification of cDNA ends system (Invitrogen, San Diego, CA) and using as a template total RNA isolated from human plantar skin (a generous gift from H. Winter, Deutsches Krebsforschungszentrum). Primers for first-round PCR were adaptor primer (5′-GGC CAC GCG TCG ACT AGT ACT TTT TTT TTT TTT TTT T) and gene-specific primer ol1353 (5′-GGC CGA ATT CAT GGC CGA AGT TCA GGG TCA GG); primers for second-round PCR were ol1353 and ol1354 (5′-GCC TCT AGA GAT TTA GAT GGA GAC GCT GTT CTC). The cDNA was cloned into the *Eco*RI and *Xba*I sites of pcDNA3 vector (Invitrogen), and the complete sequence was determined. The sequence of the isolated cDNA was almost 100% identical to the recently described variant (20), containing all but one of the described sequence variants [i.e., 561(A/G), 811(T/G), 921(G/T), 1440(T/C), 1584(C/T), 1587(T/C), 1650(A/C)] that differed from the primarily published 15-LOX-2 cDNA (21).

Catalytically inactive mutants of 15-LOX-2 and 8-LOX were generated by replacing histidines 373 and 379, respectively, by glutamine. Site-directed mutagenesis was performed using the QuikChange Site-Directed Mutagenesis Kit (Stratagene, La Jolla, CA). Primers for the 15-LOX-2$^{[H373Q]}$ mutant were ol2089 (5′-CAT GAG GCC CTC ACG CAA TTG CTG CAC TC ACA T) and ol2090 (5′-ATG TGA GTG CAG CAA TTG CGT GAG GGC CTC ATG); primers for the 8-LOX$^{[H379Q]}$ mutant were ol1722 (5′-CAT CTG CTG CAT GCC CAA TTG ATT CCA GAA GTC) and ol1723 (5′-GAC TTC TGG AAT CAA TTG GGC ATG CAG CAG ATG).

For subcloning into pRevTRE vectors, the cDNAs of wild-type and mutant 15-LOX-2 were reamplified from pcDNA3 vectors using the Expand High Fidelity PCR System (Roche Applied Science, Mannheim, Germany) and primers ol1885 (5′-GGG GGG GCT CGG ATC CAC TAG TAA) and ol1886 (5′-CGG TGC GTC GAC GGG CCC TCT AGA GAT TTA) with *Bam*HI and *Sal*I sites added in the 5′ and 3′ primers, respectively. For amplification of the 8-LOX cDNA, primers ol1883 (5′-GGG GTC TGA TCA ATC

CAC TAG TAA CGG CCG) and ol1884 (5′-GGG GGG TAG ATG CAT GCT CGA GTT AGA T) containing *Bcl*I and *Xho*I sites, respectively, were used. Upon digestion with adequate restriction enzymes, PCR amplification products were cloned into the *Bam*HI and *Sal*I sites located downstream to the Tet operator of pRevTRE vector.

The complete sequences of all constructs were determined on both strands using the ABI Big Dye Terminator Cycle Sequencing Ready Reaction Kit, and the products were resolved on an ABI prism 310 Genetic Analyzer (Perkin-Elmer/Applied Biosystems). The sequences were assembled and analyzed using the Heidelberg Unix Sequence Analysis Resources software programs.

Establishment of double-stable Tet-On keratinocyte cell lines

To establish inducible LOX expression in mouse keratinocyte cell line 308, the retroviral BD Tet-On Gene Expression System (BD Biosciences) was used according to the manufacturer's protocol with slight modifications. Briefly, Phoenix-Eco packaging cells were transiently transfected at 50–60% confluence with pRevTet-On using the calcium phosphate coprecipitation method (BD Biosciences) according to the manufacturer's instructions. After 18–20 h, cells were washed once with PBS and fresh medium was added. At 48–72 h after transfection, the virus-containing supernatant was collected and passed through a 45 μm filter, and 6 μg/ml hexadimethrine bromide (Sigma-Aldrich) was added. Ten to 15 ml of supernatant per 100 mm dish was applied to the host keratinocytes at 30–50% confluence. After 24 h, infected mouse cells were selected by 600 μg/ml G418, and surviving colonies were isolated. Clonal cell lines were tested for the capacity of Tet-On induction by transient transduction with pRevTRE-Luc retroviral supernatant obtained as described above. In one of these keratinocyte lines, luciferase expression from transiently transduced pRevTRE-Luc was undetectable in the absence of dox but was induced by ~200-fold in the presence of 2 μg/ml dox. This cell line (designated Cl20) was then used to establish clones expressing wild-type and mutant 15-LOX-2 and 8-LOX by transduction with retroviral supernatants obtained upon transfection with the corresponding pRevTRE-LOX constructs. Double-stable clones were isolated as described above using 150 μg/ml hygromycin B for selection. To induce the expression of LOX, cells were cultured in medium containing 10% serum, and 2 μg/ml dox was added at 24 h after seeding.

Cell proliferation assay

Cells plated at a density of 2.5×10^5 cells/well on six-well plates were fed 24 h later with fresh medium containing PBS (vehicle) or 2 μg/ml dox. After another 24 h, fresh medium containing 25 μM AA, 25 μM LA, 10 μM baicalein, or ethanol (vehicle) was added, and it was replaced every 48 h. Cells were harvested at different time points and washed with PBS, trypsinized, and stained with trypan blue. Living cells were counted with a hematocytometer.

BrdU incorporation assay

Cells plated on Nunc Lab-Tek eight-well glass object slides at a density of 7×10^4 cells/well were fed with fresh medium containing PBS (vehicle) or 2 μg/ml dox at 24 h after plating. At 24 h after dox induction, cells were treated in quadruplicate with various applicants [10 μM baicalein, 1 μM 8(*S*)-, 8(*R*)-, 15(*S*)-, or 15(*R*)-HETE, 1 μM 9(*S*)- or 13(*S*)-HODE, or 1 mM NAC) for 24 h and with mitogen-activated protein kinase (MAPK) inhibitors (50 μM PD98509, SB203580, or SP600125) for 4 h before BrdU labeling. After 2 h of labeling with 1 μg/μl BrdU/desoxycytosine (Roche Diagnostics), cells were fixed in 80% cold ethanol for 30 min, denaturated in 2 M HCl for 30 min, blocked with 3% ELISA-BSA (Sigma-Aldrich) in PBS for 15 min, and incubated with monoclonal anti-BrdU antibody (1:10) for 2 h followed by incubation with Cy3-conjugated goat anti-mouse IgG antiserum (1:100) including Hoechst 33258 (1:1,000) for 45 min. Object slides were mounted using DAKO® Fluorescent Mounting Medium (Dako Cytomation GmbH, Hamburg, Germany). Immunofluorescence was detected using an Axioskop 2 fluorescence microscope (Zeiss, Göttingen, Germany). The mitotic index was measured by counting the percentage of double-labeled cells in quadruplicate in four different wells.

Measurement of ROS

For measurement of ROS production, cells were washed at 48 h after dox induction with PBS, trypsinized, and incubated in 20 μM 2′,7′-dichlorofluorescein diacetate (DCF; Molecular Probes, Eugene, OR) in 1 ml of PBS for 30 min at 37°C. The fluorescence intensity was measured with a FACScan flow cytometer (Becton Dickinson, San Jose, CA) at 530 nm using the data-acquisition program CELLQuest.

Western blot analysis

Proteins (50 μg) from cell homogenates were electrophoresed on 7.5% SDS-polyacrylamide gels and electroblotted onto polyvinylidene difluoride membranes (Millipore, Bedford, MA). Equal loading/transfer was confirmed by Ponceau S staining of the membranes. Filters were blocked with 5% nonfat milk/TBS-T overnight at 4°C. Incubations with primary and secondary antibodies were performed in TBS/T containing 5% nonfat dry milk for 1 h using anti-human 15-LOX-2 antiserum (1:5,000), anti-mouse 8-LOX antiserum (1:2,000), anti-human β-actin antiserum (1:500), and the peroxidase-conjugated secondary antibodies (1:1,000). Membranes were subsequently treated as recommended by the supplier of the enhanced chemiluminescence detection system (Amersham Biosciences, Freiburg, Germany).

LOX product analysis in cells and cell-free protein extracts

LOX activity was quantified by measuring HETE and HODE formation in cells or in cell-free protein extracts. Cells plated at a density of 2.5×10^6 cells/100 mm plate were induced after 24 h with 2 μg/ml dox. Twenty-four hours later, cells were treated with 25 μM AA, 25 μM LA, 1 mM NAC, or vehicle control, and total protein homogenate was isolated 16 h later. For baicalein inhibitor studies, cells were treated 24 h after dox induction with 10 μM baicalein and labeled 12 h later with 25 μM [1-^{14}C]AA (1.85–2.29 GBq/mmol; Amersham Biosciences) for another 12 h. Lipids were extracted from cell homogenates or cell culture medium (supernatant) with a modification of the Bligh and Dyer procedure (22) as described. The final mixture, containing 1.5 ml of methanol, 1.5 ml of methylene chloride, and 1.3 ml of water, was centrifuged, and the organic phase was removed and evaporated. For subsequent saponification, the lipid fraction was cleaved by alkaline hydrolysis with 5% KOH in methanol at 60°C for 30 min under argon protection. The hydrolysis was stopped by neutralization with glacial acetic acid, and the free fatty acids were extracted with ethyl acetate. After evaporation of the organic solvent, the extracted fatty acids were dissolved in ethanol and an aqueous 0.1 M ammonium formate buffer, pH 3.1, was added to obtain a 15 vol% ethanolic solution. A fatty acid-enriched fraction was obtained by solid-phase extraction of the samples on Sep-Pak Plus C18 cartridges (Waters, Milford, MA) with ethyl acetate according to Powell (23). Products were dissolved in ethanol and stored at −70°C until further analysis.

For cell-free measurements, aliquots of 250 μg of cytosolic protein homogenates were incubated with 100 μM AA for 15 min

at 37°C. The incubations were terminated by the addition of 40 μl of 1 M sodium formate buffer (pH 3.1), and products were extracted as described above.

Products were analyzed by reverse-phase HPLC on a 5 μm YMC-Pack ODS-AM column or a 4 μm YMC-Pack ODS-H80 column (25 × 0.46 cm; YMC Europe, Schermbeck, Germany) with a 1 cm guard column using the solvent system of methanol-water-acetic acid (82:18:0.01, v/v) and a flow rate of 0.5 ml/min. Elution was monitored at 236 nm with a Bio-Tek Kontron 540 diode array detector. For measurement of labeled products, collected fractions (0.125 ml) were subjected to liquid scintillation counting.

Terminal deoxynucleotidyl transferase–mediated dUTP nick-end labeling assay

To measure apoptotic cells, the in situ cell death detection kit TMR Red (Roche Biosciences) was used. Briefly, cells plated on Nunc Lab-Tek eight-well glass object slides at a density of 7×10^4 cells/well were induced by dox (2 μg/ml), fixed 48 h later in 80% cold ethanol, and stained according to the manufacturer's instructions.

Statistical analyses

All values are presented as means ± SD. Statistical significance was evaluated using Student's *t*-test, with $P < 0.05$ considered statistically significant.

RESULTS

Generation of LOX-inducible mouse keratinocyte lines

Previous attempts to isolate stable clones overexpressing 15-LOX-2 or 8-LOX in primary keratinocytes or various nontumorigenic keratinocyte lines failed, indicating that expression of these LOXs may prevent clonal expansion. Therefore, we used a Tet-inducible system to compare the biological effects of 15-LOX-2 and 8-LOX expression in keratinocytes. The benign papilloma-producing mouse keratinocyte cell line 308 was used for stable expression of rtTA (reverse Tet repressor) by infection with pRevTet-On virus. Various clones were transiently infected with pRevTRE-Luc, and Tet-On induction was determined. Clone 20 (Cl20) showed the strongest induction of luciferase activity in the presence of dox, with only marginal background in the absence of the drug (data not shown). This clone was selected for further infection with different pRevTRE virus constructs. Wild-type and mutant 15-LOX-2 and 8-LOX coding regions were cloned into pRevTRE, and double-stable inducible expression lines were obtained by virus infection. Several clones were analyzed for LOX induction upon dox treatment and compared with the parental cell lines 308

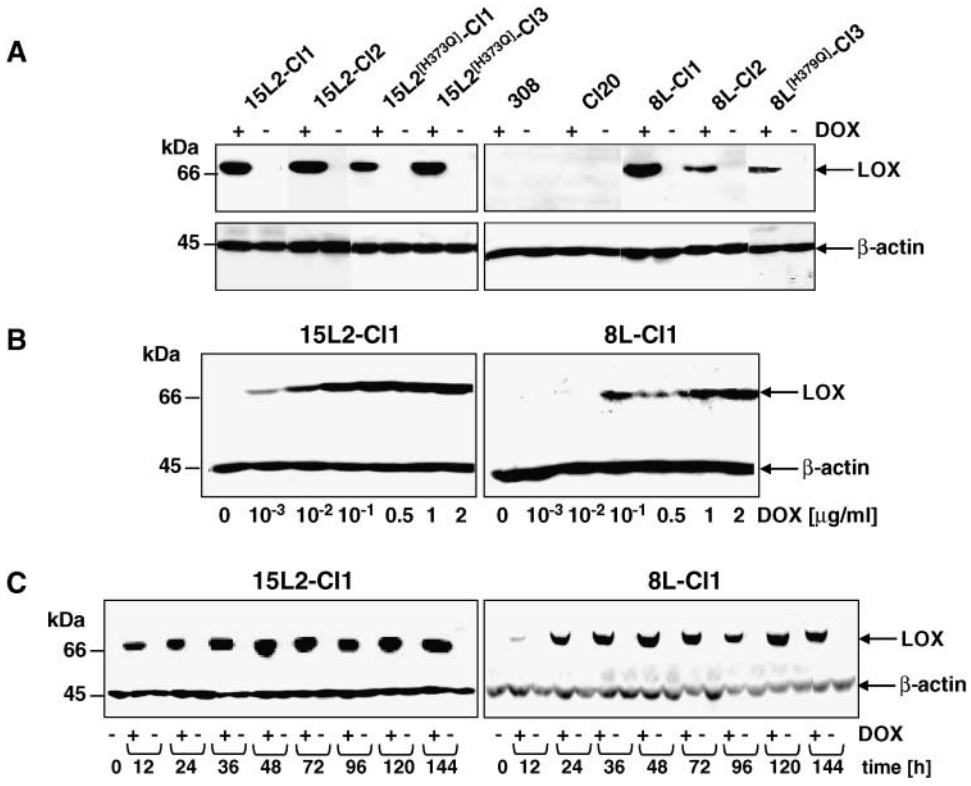

Fig. 1. Inducible expression of 15-lipoxygenase (LOX)-2 and 8-LOX in mouse keratinocytes. A: Double-stable transfectants expressing 15-LOX-2, 8-LOX, or inactive mutant protein as well as the parental mouse keratinocyte cell line 308 and the transactivator cell line Cl20 were treated with 2 μg/ml doxycycline (dox) in culture medium for 48 h, and LOX expression level was measured by Western blotting using antibodies against 15-LOX-2 (left panel) and 8-LOX (right panel). β-Actin was used as a control for equal loading. B: 15L2-Cl1 and 8L-Cl1 cells were treated with the indicated concentrations of dox for 48 h, and LOX expression was measured by Western blotting. C: 15L2-Cl1 and 8L-Cl1 cells were treated with 2 μg/ml dox for the indicated periods of time, and the levels of LOX were measured by Western blotting.

and the rtTA-expressing Cl20, in which LOX expression was not detectable (**Fig. 1A**). Clones that gave similar protein expression levels for 15-LOX-2 (15L2-Cl1 and the corresponding inactive mutant 15L2$^{[H373Q]}$-Cl3) and 8-LOX (8L-Cl1 and the corresponding inactive mutant 8L$^{[H379Q]}$-Cl3) were used throughout these studies (Fig.1A). In 15L2-Cl1 and 8L-Cl1 cells, 15-LOX-2 and 8-LOX expression, respectively, increased in a dose-dependent manner in response to dox, whereas no LOX expression was detectable in the absence of the drug (Fig. 1B). Dox-induced LOX ex-

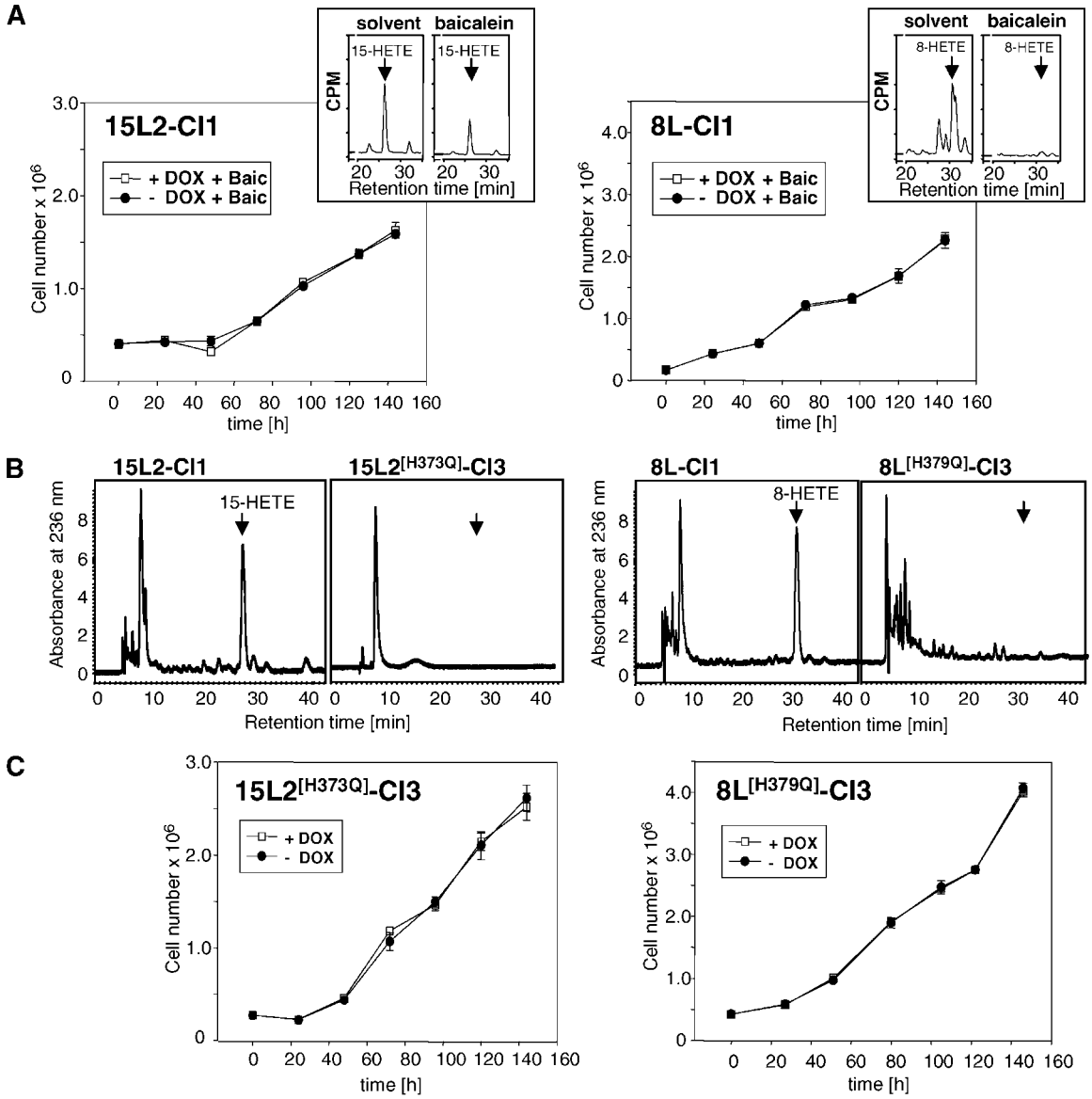

Fig. 2. LOX enzyme activity is required for growth inhibition. A: 15L2-Cl1 and 8L-Cl1 cells were plated at 2.5 × 10^5 cells/six-well plate in culture medium and induced 24 h later with 2 μg/ml dox or vehicle control in the presence or absence of 10 μM baicalein. Medium was changed every 2 days. The number of living cells at each time point was counted by a hematocytometer. The data shown are means ± SD of three wells counted in triplicate. Experiments were repeated two times with similar results. Inset: Cells were treated 24 h after dox induction with 10 μM baicalein and labeled 12 h later with 25 μM [1-^{14}C]arachidonic acid (AA) for another 12 h. Total lipids were extracted from cell supernatants with methanol-dichloromethane (1:1, v/v), dried under vacuum, redissolved in methanol-water-acetic acid (82:18:0.01, v/v), injected on a 5 μm YMC-Pack ODS column, and eluted at 0.5 ml/min. Collected fractions (0.125 ml) were subjected to liquid scintillation counting. Authentic 15-hydroxyeicosatetraenoic acid (HETE) and 8-HETE were used as standards. B: Reverse-phase HPLC analysis of products formed in cell extracts from keratinocyte lines expressing wild-type (15L2-Cl1, 8L-Cl1) or mutant (15L2$^{[H373Q]}$-Cl3, 8L$^{[H379Q]}$-Cl3) LOX protein. Homogenates from cells grown in the presence of 2 μg/ml dox for 48 h were incubated in 10 mM Tris-HCl, 1 mM EDTA, pH 7.4 buffer with 100 μM AA for 15 min at 37°C. Products were extracted with methanol-dichloromethane (1:1, v/v), dried under vacuum, redissolved in methanol-water-acetic acid (82:18:0.01, v/v), injected on a 5 μm YMC-Pack ODS-AM column, and eluted at 0.5 ml/min. The eluate was monitored at 236 nm. Authentic 15-HETE and 8-HETE were used as standards. The retention times of 15-HETE and 8-HETE were 26.3 and 31.5 min, respectively. C: Induction of inactive 15-LOX-2 and 8-LOX protein has no effect on cell growth. Growth of 15L2$^{[H373Q]}$-Cl3 and 8L$^{[H379Q]}$-Cl3 cells was measured as described for A. The data shown are means ± SD of three wells counted in triplicate. Experiments were repeated two times with similar results.

pression was rapid and persistent, being detectable as early as 12 h after induction and reaching a plateau between 24 and 144 h after treatment (Fig. 1C). Induction of LOX expression correlated with highly increased production of 8-HETE and 15-HETE (**Fig. 2A**, inset, B). The majority (95%) of the LOX products were detected in the cell supernatant, whereas 5% were found in cell extracts. The ratio of free to phospholipid-bound LOX products was ~10:1.

Forced expression of 15-LOX-2 and 8-LOX inhibits the growth of premalignant mouse keratinocytes

To study the effects of 15-LOX-2 and 8-LOX expression on 308 keratinocyte proliferation, 15L2-Cl1 or 8L-Cl1 cells and Cl20 control cells were treated with dox, and the total cell number was assessed every 24 h. Both 15L2-Cl1 or 8L-Cl1 cells showed a decline in proliferation in response to dox-induced LOX expression, whereas the proliferation of Cl20 cells was unaffected by the drug (**Fig. 3A**). The inhibitory effect of dox-induced LOX expression was detected earlier in 8L-Cl1 cells compared with 15L2-Cl1 cells but reached similar levels of ~30–40% inhibition by 96–144 h.

15-LOX-2- and 8-LOX-induced growth inhibition is associated with the inhibition of DNA synthesis

Terminal deoxynucleotidyl transferase–mediated dUTP nick-end labeling assays indicated that the 15-LOX-2- and 8-LOX-induced growth inhibition in 308 keratinocytes was not attributable to increased apoptosis. Likewise, induction of LOX expression did not alter the expression of apoptosis-related proteins such as bcl2 and bax (data not shown). The induction of terminal differentiation was excluded by the absence of detectable expression of keratins 1 and 10, fillagrin, and loricrin. To assess the effects of LOX expression on DNA synthesis, BrdU labeling was determined at different time points after induction of

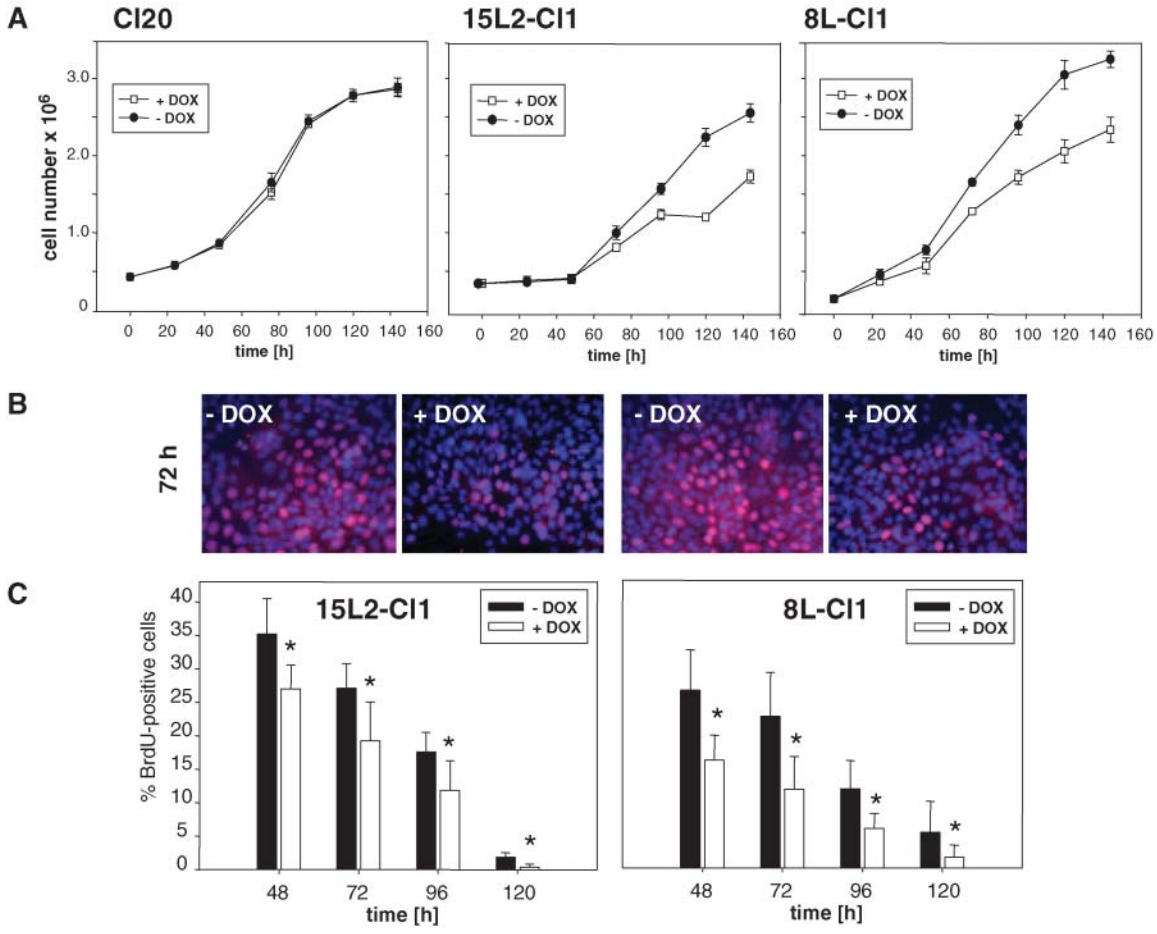

Fig. 3. 15-LOX-2 and 8-LOX expression induces the inhibition of cell growth and 5-bromo-2-deoxy-uridine (BrdU) incorporation. A: Cl20, 15L2-Cl1, and 8L-Cl1 cells were plated at 2.5×10^5 cells/six-well plate in culture medium and 24 h later induced with 2 μg/ml dox or vehicle control. Media were changed every 2 days. The number of living cells at each time point was counted by hematocytometer. The data shown are means ± SD of at least two independent experiments, each carried out in triplicate. B: BrdU incorporation. Cells plated at 7×10^4 cells/chamber were labeled at 72 h after dox induction with BrdU for 2 h. Cells were fixed and analyzed for immunofluorescence using monoclonal anti-BrdU antibody followed by Cy3-conjugated anti-mouse immunoglobulin. Nuclei were counterstained with Hoechst dye 33258. C: BrdU incorporation assays were conducted at different time points after dox induction. DNA synthesis is expressed as a percentage of BrdU-positive cells. In total, 10,000 cells were counted in each experiment. Data represent means ± SD of four wells counted in quadruplicate. Experiments were repeated three times with similar results. * $P < 0.03$ (Student's *t*-test).

15-LOX-2 and 8-LOX expression by quantifying BrdU-positive cells by fluorescence microscopy. Although no difference was observed in Cl20 cells, dox application significantly reduced the percentage of S-phase cells in 15L2-Cl1 and 8L-Cl1 clones. Inhibition of BrdU incorporation was stronger at earlier time points in 8L-Cl1 cells compared with 15L2-Cl1 cells but reached similar levels by 120 h, yielding 70–80% inhibition (Fig. 3B, C).

LOX enzyme activity is required for growth inhibition

Bhatia et al. (24) recently showed that the biological effects of 15-LOX-2 are not necessarily dependent on enzyme activity. To assess whether enzyme activity was required for the LOX-induced growth inhibition in keratinocytes, we examined the effects of the LOX inhibitor baicalein. In the LOX-expressing keratinocyte clones, 10 μM baicalein almost completely blocked the dox-induced accumulation of 8-HETE and reduced the production of 15-HETE by 50%, as measured in the supernatants of the cells at 48 h after induction (Fig. 2A, inset). Whereas no effect of baicalein was observed on growth in Cl20 cells (data not shown), the dox-induced growth inhibition was completely abrogated by baicalein in both 15L2-Cl1 and 8L-Cl1 cells (Fig. 2A). Replacing one of the three absolutely conserved histidines (histidine 373 in 15-LOX-2 and histidine 379 in 8-LOX) by glutamine by means of site-directed mutagenesis resulted in the complete loss of catalytic activity for the mutant enzymes (Fig. 2B). Although double-stable expression clones of the LOX mutants exhibited high levels of dox-induced protein expression (Fig. 1B), no effect of dox was observed on the proliferation of these cells (Fig. 2C). Together, these data show that the growth-inhibitory effects of both LOXs depend on enzyme activity.

Opposing effects of AA and LA on dox-induced growth inhibition

15-LOX-2 has been shown to accept both AA and LA as substrates, whereas 8-LOX metabolizes LA less efficiently. To examine the contribution of both LOX substrates to the growth-inhibitory effects, LOX expression was induced in the presence of exogenous AA or LA. In the dose range tested (6–25 μM), AA did not affect the growth of non-induced 15L2-Cl1 cells but dose-dependently increased

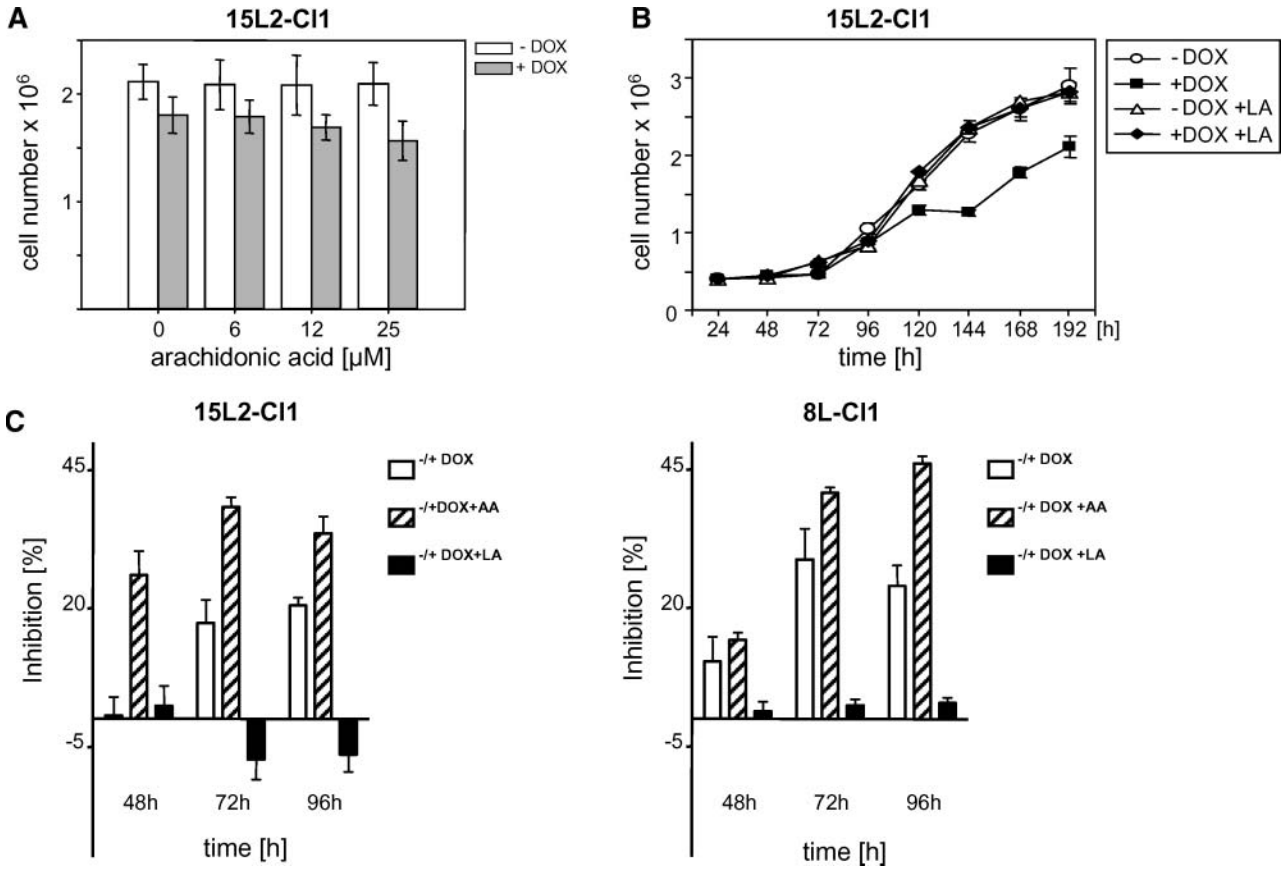

Fig. 4. Opposing effects of AA and linoleic acid (LA) on dox-induced growth inhibition. Cells plated at 2.5×10^4 cells/six-well plates in culture medium were induced by 2 μg/ml dox after 24 h and treated 24 h later with AA, LA, or vehicle control. A: Cells were treated with different concentrations of AA as indicated for 48 h, and the numbers of living cells were determined. B: Cells were treated with 25 μM LA, and the numbers of living cells were determined at different time points. C: Cells were treated with 25 μM AA, 25 μM LA, or vehicle control for different times as indicated. The numbers of living cells were determined, and the percentage of growth inhibition was calculated compared with vehicle control-treated cells. The data shown are means ± SD of three wells counted in triplicate and represent one of two experiments yielding similar results.

the dox-induced growth inhibition at 48 h after treatment (**Fig. 4A**). Likewise, LA at dose of 25 μM had no effect on the growth of noninduced 15L2-Cl1 cells but abolished the dox-induced growth inhibition (Fig. 4B). The increase of the dox-dependent growth inhibition in the presence of 25 μM AA and its reversion by 25 μM LA were observed in both 15L2-Cl1 and 8L-Cl1 cells at various time points (Fig. 4C). Induction of 15-LOX-2 in the presence of LA led to an increase of 13-HODE formation without changing the basal level of 15-HETE obtained in the absence of AA (**Fig. 5**).

Effects of exogenous LOX products on the proliferation of 308 keratinocytes

We then wanted to determine whether exogenously added AA and LA metabolites of 15-LOX-2 and 8-LOX could affect keratinocyte proliferation. Mutant $15L2^{[H373Q]}$-Cl3 cells were treated in the absence of dox with 1 μM 15*S*-HETE, 8*S*-HETE, 13*S*-HODE, or 9*S*-HODE. DNA synthesis was measured at various time points after treatment. 8*S*-HETE strongly and persistently inhibited BrdU incorporation by ~80%, whereas inhibition by 15*S*-HETE was less pronounced at earlier time points but reached similar levels at 96 and 120 h (**Fig. 6A**, left panel). 13*S*-HODE and 9*S*-HODE treatment, in contrast, did not significantly affect cell proliferation (Fig. 6A, right panel). Possible stereospecificity of the HETE effects was examined by comparing the effects of exogenous 8*S*- or 15*S*-HETE versus 8*R*- or 15*R*-HETE. The inhibition of BrdU incorporation was ~5-fold greater for 8*S*- and ~3-fold greater for 15*S*- than for the corresponding *R* enantiomers (Fig. 6B).

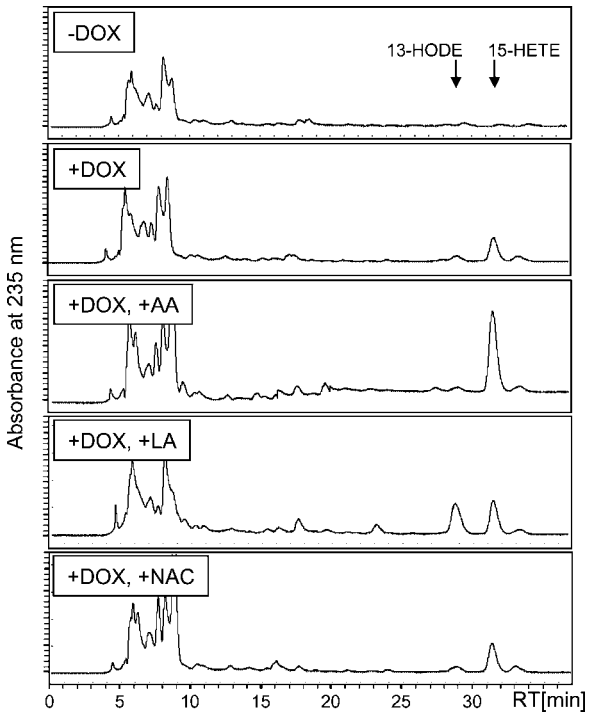

Fig. 5. Production of HETEs and hydroxyoctadecadienoic acid (HODEs) in 15-LOX-2-expressing mouse keratinocytes. 15L2-Cl1 cells were plated in culture medium at 2.5×10^6 cells/100 mm dish and induced 24 h later with 2 μg/ml dox or vehicle control (−DOX). Twenty-four hours later, cells were treated with 25 μM AA, 25 μM LA, 1 mM *N*-acetyl-L-cysteine (NAC), or vehicle control (+DOX) for 16 h. The culture medium was accurately removed, and total lipids were extracted from cell sonicates with methanol-dichloromethane (1:1, v/v), dried under vacuum, redissolved in methanol-water-acetic acid (82:18:0.01, v/v), injected on a 4 μm YMC-Pack ODS-H80 column, and eluted at 0.5 ml/min. The eluate was monitored at 236 nm. Authentic 15-HETE and 13-HODE were used as standards. The retention times (RT) of 13-HODE and 15-HETE were 28.8 and 31.4 min, respectively. Representative data are given from three independent experiments with similar results.

Generation of ROS is critically involved in the LOX-mediated growth inhibition

Increased LOX activity is known to be a rich source of ROS generated as by-products during oxygenation and oxidative degradation of the polyunsaturated fatty acids. Recently, increased generation of ROS was shown to be critically involved in 5-LOX-induced growth arrest in primary fibroblasts (25). To investigate whether ROS may play a role in 15-LOX-2- and 8-LOX-induced growth inhibition, we analyzed the effects of antioxidant treatment on cell growth. 15L2-Cl1 or 8L-Cl1 cells were preincubated in medium containing 1 mM NAC for 24 h and induced by dox, and BrdU incorporation was measured at 48 and 72 h later. As seen in **Fig. 7**, NAC treatment abolished the dox-induced inhibition of BrdU incorporation in both 15L2-Cl1 and 8L-Cl1 cells, even though NAC did not suppress the production of 15-HETE (Fig. 5). This result indicates that ROS generation may be involved in the LOX effects in 308 cells. Therefore, we analyzed the ROS status of the LOX-expressing 308 clones either in the presence or absence of dox. Levels of intracellular ROS were quantified using DCF as a fluorescence ROS indicator. Flow cytometry analysis showed significant increases in intracellular ROS levels in dox-induced 15-LOX-2- and 8-LOX-expressing 308 cells compared with noninduced cells, whereas in the 308 parental cells, dox treatment did not affect intracellular ROS generation (**Fig. 8**).

p38 MAPK signaling pathway is involved in LOX-mediated growth inhibition

We next wanted to investigate the potential signaling cascades involved in LOX-mediated growth inhibition. The MAPK signaling pathway has been implicated in LOX signaling in various cell types (26, 27). To investigate the role of MAPK in LOX-induced effects in 308 cells, we used pharmacological inhibitors to attenuate signaling via these kinases. Sixty hours after dox induction, 15-LOX-2- and 8-LOX-expressing cells were incubated in medium containing 50 μM of specific inhibitors for c-Jun N-terminal kinase (JNK) (SP600125), p38 kinase (SB203850), or extracellular signal-regulated kinase (ERK) (PD98059), and BrdU incorporation was measured 4 h later. Whereas the inhibition of ERK and JNK did not show a significant effect on the dox-induced reduction of BrdU incorporation, treatment of the cells with the specific p38 kinase inhibitor completely abrogated dox-induced growth in-

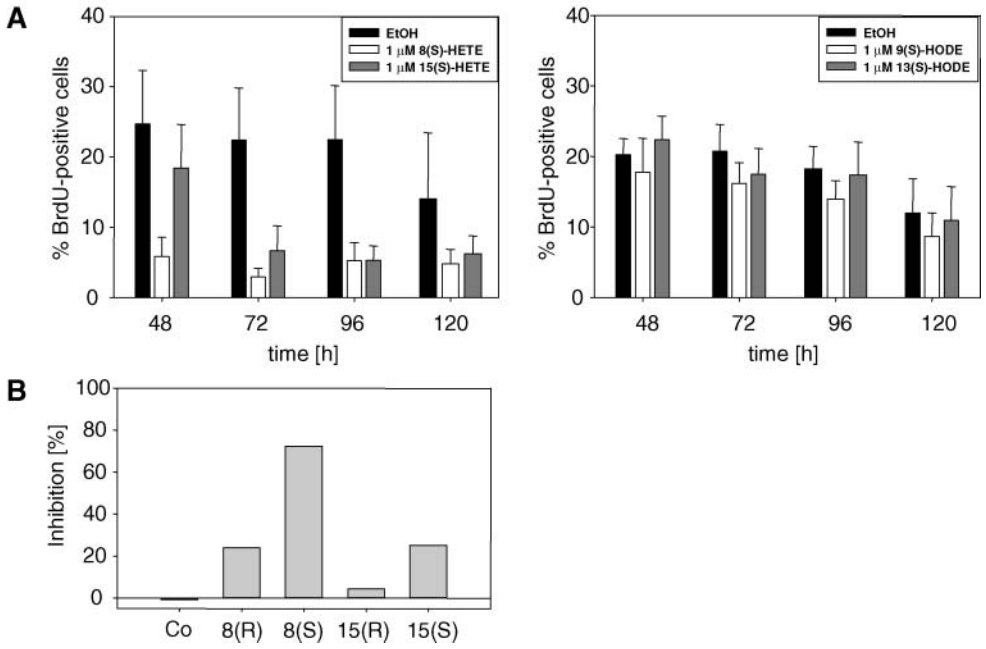

Fig. 6. Effects of exogenous HETEs and HODEs on the proliferation of mouse keratinocytes. A: 15L2$^{[H373Q]}$-Cl3 mouse keratinocytes were plated in culture medium at 7×10^4 cells/eight-well slide and incubated 24 h later in the presence of ethanol (EtOH) or 1 μM 8(*S*)-HETE, 15(*S*)-HETE, 9(*S*)-HODE, or 13(*S*)-HODE. BrdU incorporation assays were conducted at the indicated time points, and the percentage of BrdU-positive cells was calculated as described in Materials and Methods. B: 15L2$^{[H373Q]}$-Cl3 cells were grown in the presence of vehicle (Co) or 1 μM 8(*S*)-, 8(*R*)-, 15(*S*)-, or 15(*R*)-HETE for 48 h. BrdU incorporation assays were conducted, and the percentage of growth inhibition compared with vehicle-treated cells was calculated. The data shown are means ± SD of three wells counted in triplicate and represent one of two experiments yielding similar results.

hibition in both 15-LOX-2- and 8-LOX-expressing cells (**Fig. 9**).

DISCUSSION

There is still a considerable discrepancy between the knowledge of the structural biology of mammalian LOXs and the biological relevance of LOX activity and the functional importance of LOX products. In addition, some evidence suggests functions of LOX outside of the AA cascade, in that not only free PUFAs are a substrate for lipoxygenation reactions (6, 28–30). In addition, there are recent indications for functions of LOX that are independent of the enzymatic activity of individual LOXs (24, 31).

Yet, less information is available for the functions of epidermis-type LOXs, including the pair of orthologous epidermal 8-LOX and 15-LOX-2, which combine high

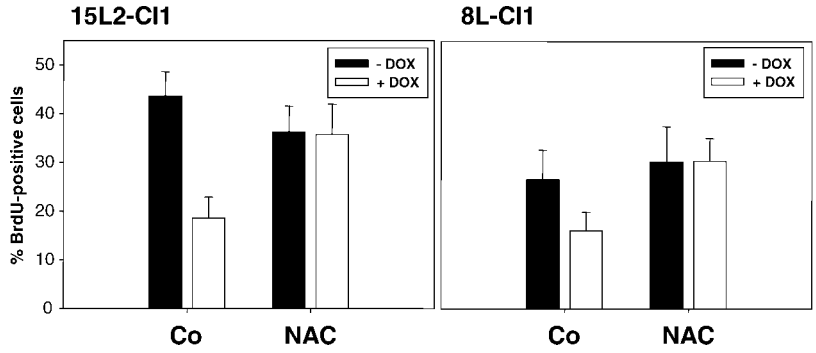

Fig. 7. Antioxidant reverses dox-induced inhibition of DNA synthesis in 15-LOX-2- and 8-LOX-expressing mouse keratinocytes. 15L2-Cl1 and 8L-Cl1 cells plated in culture medium at 7×10^4 cells/eight-well slide were induced 24 h later by 2 μg/ml dox and treated 24 h later with 1 mM NAC or vehicle control (Co). BrdU incorporation assays were conducted after 48 h, and the percentage of BrdU-positive cells was calculated as described in Materials and Methods. In total, 10,000 cells were counted in each experiment. The data shown are means ± SD of four wells counted in quadruplicate and represent one of two experiments yielding similar results.

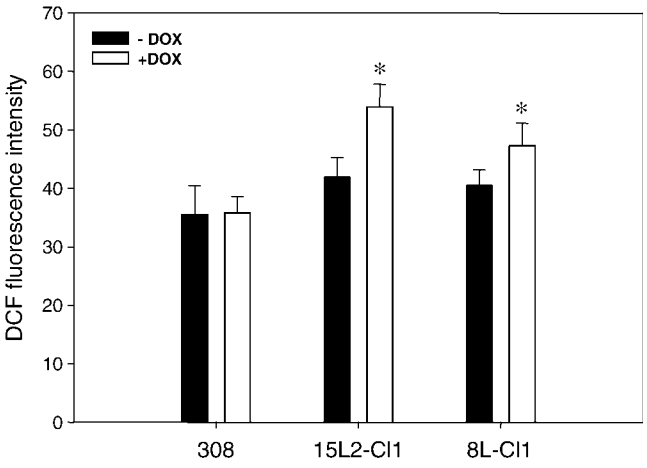

Fig. 8. Increased reactive oxygen species (ROS) levels in 15-LOX-2- and 8-LOX-expressing mouse keratinocytes. Cells were grown in culture medium for 48 h in the presence or absence of 2 μg/ml dox, and ROS levels were measured by flow cytometry analysis of 2′,7′-dichlorofluorescein diacetate (DCF)-labeled cells. Data represent means ± SD of six samples. * $P < 0.03$ (Student's *t*-test).

structural identity with differential epidermal expression (14, 15) and a differing product spectrum: 8*S*-HETE and 9*S*-HODE (16) versus 15*S*-HETE and 13*S*-HODE (21). To explore the functions of these LOXs in keratinocytes, we established inducible expression lines and analyzed the effects of 8-LOX and 15-LOX-2 induction compared with the parental cell line 308 and the reverse Tet repressor expressing Cl20. 308 keratinocytes represent a cell line that was derived from mouse skin initiated with 7,12-dimethylbenz[a]anthracene and produces papillomas when grafted on athymic mice (19). The parental cells did not express 8-LOX or 15-LOX-2. We chose an inducible expression system because neither primary keratinocytes nor nontumorigenic keratinocytes retained the capacity to grow when 8-LOX or 15-LOX-2 was stably expressed. This holds true for 308 keratinocytes (data not shown) and another papilloma cell line, MT1/2, carrying the 8-LOX transgene, which decreased growth and lost the transgene after two to three passages (32). As shown here, the induction of either 8-LOX or 15-LOX-2 did indeed decrease the growth rate in both expression lines compared with parental 308 and Cl20 control cells. Induction of 8-LOX or 15-LOX-2 expression and activity strictly depended on treatment with dox. In contrast to MT1/2 papilloma cells, which, upon stable expression of 8-LOX, transiently developed morphological signs of terminal differentiation and expressed keratin 1 (32), the reduced proliferation capacity of 308 cells induced by 8-LOX or 15-LOX-2 expression was not attributable to the stimulation of differentiation, as supported by the complete absence of keratin 1 and keratin 10 expression as well as other differentiation markers in dox-treated cells. In fact, we could not detect the expression of PPARα in either 308 parental cells or the 308-derived LOX expression lines. Activation of PPARα, however, was found to be critically involved in the 8*S*-HETE induction of keratin 1 expression and differentiation in primary keratinocytes (33). 15*S*-HETE was previously shown to suppress the proliferation of prostatic and colorectal cancer cells, an effect that was mediated by the activation of PPARγ (26, 34, 35). However, neither the parental 308 keratinocytes nor the LOX-expressing lines expressed PPARγ, thus ruling out this pathway for the LOX-induced growth inhibition. Likewise, induction of 8-LOX or 15-LOX-2 expression did not induce apoptosis in these cells, as shown by a negative Terminal deoxynucleotidyl

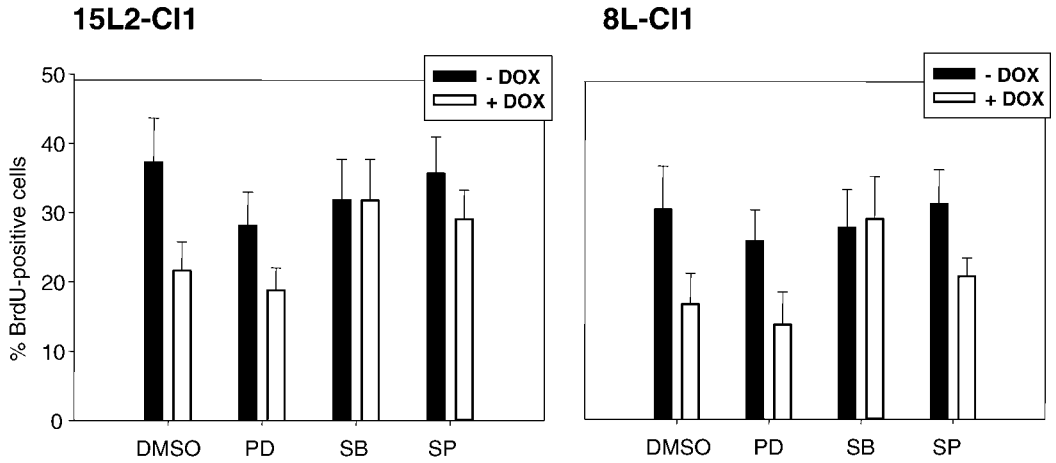

Fig. 9. Effects of specific kinase inhibitors on DNA synthesis in 15-LOX-2- and 8-LOX-expressing keratinocytes. 15L2-Cl1 and 8L-Cl1 cells were plated in culture medium at 7×10^4 cells/eight-well slide and incubated 24 h later in the presence of 2 μg/ml dox or vehicle control for 60 h. Cells were preincubated for 4 h in medium containing 50 μM specific inhibitors for c-Jun N-terminal kinase (SP600125), p38 kinase (SB203850), or extracellular signal-regulated kinase (PD98059) before BrdU incorporation assays were conducted. The percentage of BrdU-positive cells was calculated as described in Materials and Methods. In total, 10,000 cells were counted in each experiment. Data represent means ± SD of three independent experiments, each evaluated in quadruplicate from four independent visual fields.

transferase–mediated dUTP nick-end labeling assay and the lack of an effect on the expression of apoptosis-related proteins such as bcl2 and bax. These results exclude apoptosis as a cause for the reduced growth rate of the expression lines, although an apoptosis-inducing activity of 15*S*-HETE was observed in human cornea epithelial cells (36). Moreover, we did not observe senescence (data not shown) as a consequence of the induction of 8-LOX or 15-LOX-2 expression. Such an effect was observed in human prostatic epithelial cells upon ectopic expression of 15-LOX-2 (24). Forced expression of 8-LOX in CH72 carcinoma cells was previously found to reduce the growth capacity of the stable transfectants, an effect that was attributed to a G1 block (32). This was not observed in 308 cells upon induction of either 8-LOX or 15-LOX-2 expression. Together, these data show that induced or permanent expression of either 8-LOX or 15-LOX-2 in epithelial cells commonly inhibits proliferation along cell-specific pathways.

The BrdU labeling experiments clearly documented that in 308 keratinocytes, the inhibition of DNA synthesis is responsible for the observed reduction of cell growth by induction of 8-LOX or 15-LOX-2 expression and activity. Inhibition of DNA synthesis could be recapitulated by treatment of keratinocytes with either 1 μM 8*S*-HETE or 1 μM 15*S*-HETE. The view that DNA synthesis is targeted by induction of 8-LOX and 15-LOX-2 in 308 cells is confirmed by the observation that suppression of LOX activities with the LOX inhibitor baicalein or the ablation of LOX activity by site-directed mutagenesis prevented both the inhibition of DNA synthesis and the production of 8-HETE or 15-HETE. This indicates a cause-and-effect relationship between the induction of 8-LOX and 15-LOX-2 expression and activity and the inhibition of DNA synthesis. Exogenously added AA significantly increased the growth-reducing activity of induced 8-LOX and 15-LOX-2 expression, which correlated with increased 8-HETE or 15-HETE formation. Interestingly, the presence of exogenous LA counteracted the LOX-induced growth inhibition. In 15-LOX-2-expressing cells, this effect is associated with an increased production of 13-HODE without changing the formation of 15-HETE. Although 9*S*- and 13*S*-HODE, the LA-derived products of 8- and 15-LOX, did not exhibit growth-modulating activities in 308 cells, it remains to be established in ongoing experiments whether or not 13-HODE is able to reverse 15-LOX-2 growth inhibition.

Both 8-HETE and 15-HETE induced growth-inhibitory effects that showed stereospecificity, as the *S* enantiomers exhibited 3- to 5-fold higher activity. This stereoselective activity suggests that receptor-mediated signaling cascades are involved in LOX-induced growth inhibition. Indeed, activation of different MAPK cascades has been shown to be involved in HETE-mediated growth regulation in various cell types, including the downregulation of ERK1/2 by 15-HETE in prostate carcinoma cells (26) and the activation of p38 MAPK by 15-HETE in human breast carcinoma cells (27). A critical role of p38 MAPK in the 8-LOX- and 15-LOX-2-induced effects is indicated by the observation that a specific inhibitor of the p38 kinase, but not of the ERK1/2 or JNK/stress-activated kinases, was able to abolish the dox-induced growth inhibition in LOX-expressing cells. p38 MAPK activation has been found to be associated with stress-induced effects, including S-phase growth arrest in Cr(VI)-exposed HeLa cells (37) and in ultraviolet B-irradiated keratinocytes (38). The ultraviolet B effect was mediated by the generation of endogenous ROS.

The 8-LOX- and 15-LOX-2-induced inhibition of DNA synthesis also was associated with increased ROS levels. Suppression of ROS formation by NAC reversed the growth-inhibitory activity. NAC, however, did not inhibit 15-HETE formation in 15-LOX-2-expressing cells, suggesting that ROS are downstream mediators of HETE-induced growth inhibition. In fact, this radical scavenger has been shown to scavenge ROS generated in the course of the reduction of fatty acid hydroperoxides such as 8- and 15-HPETE (25) without inhibiting the LOX reaction per se (39). Thus, both lipid-mediated and ROS-mediated effects may contribute to the activation of p38 MAPK and the inhibition of growth.

In conclusion, our data indicate that 15-LOX-2 and 8-LOX, although displaying different positional specificity, may use common signaling pathways to induce growth inhibition in premalignant epithelial cells.

The excellent technical assistance of Brigitte Steinbauer and Ina Kutschera is gratefully acknowledged. The authors thank Dr. H. Winter for providing human RNA samples.

REFERENCES

1. Brash, A. R. 1999. Lipoxygenases: occurrence, functions, catalysis, and acquisition of substrate. *J. Biol. Chem.* **274:** 23679–23682.
2. Marks, F., and G. Furstenberger. 2000. Cancer chemoprevention through interruption of multistage carcinogenesis. The lessons learnt by comparing mouse skin carcinogenesis and human large bowel cancer. *Eur. J. Cancer.* **36:** 314–329.
3. Uchida, K. 2003. 4-Hydroxy-2-nonenal: a product and mediator of oxidative stress. *Prog. Lipid Res.* **42:** 318–343.
4. Kuhn, H., and B. J. Thiele. 1999. The diversity of the lipoxygenase family. Many sequence data but little information on biological significance. *FEBS Lett.* **449:** 7–11.
5. Kinzig, A., M. Heidt, G. Fürstenberger, F. Marks, and P. Krieg. 1999. cDNA cloning, genomic structure and chromosomal localization of a novel murine epidermis-type lipoxygenase. *Genomics.* **58:** 158–164.
6. Yu, Z., C. Schneider, W. E. Boeglin, L. J. Marnett, and A. R. Brash. 2003. The lipoxygenase gene ALOXE3 implicated in skin differentiation encodes a hydroperoxide isomerase. *Proc. Natl. Acad. Sci. USA.* **100:** 9162–9167.
7. Krieg, P., M. Heidt, M. Siebert, A. Kinzig, F. Marks, and G. Furstenberger. 2002. Epidermis-type lipoxygenases. *Adv. Exp. Med. Biol.* **507:** 165–170.
8. Krieg, P., F. Marks, and G. Furstenberger. 2001. A gene cluster encoding human epidermis-type lipoxygenases at chromosome 17p13.1: cloning, physical mapping, and expression. *Genomics.* **73:** 323–330.
9. Brash, A. R., M. Jisaka, W. E. Boeglin, and M. S. Chang. 1999. Molecular cloning of a second human 15S-lipoxygenase and its murine homologue, an 8S-lipoxygenase. Their relationship to other mammalian lipoxygenases. *Adv. Exp. Med. Biol.* **447:** 29–36.
10. Jisaka, M., R. B. Kim, W. E. Boeglin, L. B. Nanney, and A. R. Brash. 1997. Molecular cloning and functional expression of a phorbol ester-inducible 8S-lipoxygenase from mouse skin. *J. Biol. Chem.* **272:** 24410–24416.

11. Krieg, P., A. Kinzig, M. Heidt, F. Marks, and G. Furstenberger. 1998. cDNA cloning of a 8-lipoxygenase and a novel epidermis-type lipoxygenase from phorbol ester-treated mouse skin. *Biochim. Biophys. Acta.* **1391:** 7–12.
12. Brash, A. R., W. E. Boeglin, and M. S. Chang. 1997. Discovery of a second 15S-lipoxygenase in humans. *Proc. Natl. Acad. Sci. USA.* **94:** 6148–6152.
13. Jisaka, M., R. B. Kim, W. E. Boeglin, and A. R. Brash. 2000. Identification of amino acid determinants of the positional specificity of mouse 8S-lipoxygenase and human 15S-lipoxygenase-2. *J. Biol. Chem.* **275:** 1287–1293.
14. Heidt, M., G. Fürstenberger, S. Vogel, F. Marks, and P. Krieg. 2000. Diversity of murine lipoxygenases: identification of a subfamily of epidermal isoenzymes exhibiting a differentiation-dependent mRNA expression pattern. *Lipids.* **35:** 701–707.
15. Shappell, S. B., D. S. Keeney, J. Zhang, R. Page, S. J. Olson, and A. R. Brash. 2001. 15-Lipoxygenase-2 expression in benign and neoplastic sebaceous glands and other cutaneous adnexa. *J. Invest. Dermatol.* **117:** 36–43.
16. Burger, F., P. Krieg, A. Kinzig, B. Schurich, F. Marks, and G. Furstenberger. 1999. Constitutive expression of 8-lipoxygenase in papillomas and clastogenic effects of lipoxygenase-derived arachidonic acid metabolites in keratinocytes. *Mol. Carcinog.* **24:** 108–117.
17. Furstenberger, G., F. Marks, and P. Krieg. 2002. Arachidonate 8(S)-lipoxygenase. *Prostaglandins Other Lipid Mediat.* **68–69:** 235–243.
18. Kilty, I., A. Logan, and P. J. Vickers. 1999. Differential characteristics of human 15-lipoxygenase isozymes and a novel splice variant of 15S-lipoxygenase. *Eur. J. Biochem.* **266:** 83–93.
19. Strickland, J. E., D. A. Greenhalgh, A. Koceva-Chyla, H. Hennings, C. Restrepo, M. Balaschak, and S. H. Yuspa. 1988. Development of murine epidermal cell lines which contain an activated rasHa oncogene and form papillomas in skin grafts on athymic nude mouse hosts. *Cancer Res.* **48:** 165–169.
20. Tang, S., B. Bhatia, C. J. Maldonado, P. Yang, R. A. Newman, J. Liu, D. Chandra, J. Traag, R. D. Klein, S. M. Fischer, et al. 2002. Evidence that arachidonate 15-lipoxygenase 2 is a negative cell cycle regulator in normal prostate epithelial cells. *J. Biol. Chem.* **277:** 16189–16201.
21. Brash, A. R., W. E. Boeglin, and M. S. Chang. 1997. Discovery of a second 15S-lipoxygenase in humans. *Proc. Natl. Acad. Sci. USA.* **94:** 6148–6152.
22. Bligh, E. G., and W. J. Dyer. 1959. A rapid method of total lipid extraction and purification. *Can. J. Biochem. Physiol.* **37:** 911–917.
23. Powell, W. S. 1982. Rapid extraction of arachidonic acid metabolites from biological samples using octadecylsilyl silica. *Methods Enzymol.* **86:** 467–477.
24. Bhatia, B., S. Tang, P. Yang, A. Doll, G. Aumueller, R. A. Newman, and D. G. Tang. 2005. Cell-autonomous induction of functional tumor suppressor 15-lipoxygenase 2 (15-LOX2) contributes to replicative senescence of human prostate progenitor cells. *Oncogene.* **24:** 3583–3595.
25. Catalano, A., S. Rodilossi, P. Caprari, V. Coppola, and A. Procopio. 2005. 5-Lipoxygenase regulates senescence-like growth arrest by promoting ROS-dependent p53 activation. *EMBO J.* **24:** 170–179.
26. Hsi, L. C., L. C. Wilson, and T. E. Eling. 2002. Opposing effects of 15-lipoxygenase-1 and -2 metabolites on MAPK signaling in prostate. Alteration in peroxisome proliferator-activated receptor gamma. *J. Biol. Chem.* **277:** 40549–40556.
27. Nony, P. A., S. B. Kennett, W. C. Glasgow, K. Olden, and J. D. Roberts. 2005. 15S-Lipoxygenase-2 mediates arachidonic acid-stimulated adhesion of human breast carcinoma cells through the activation of TAK1, MKK6, and p38 MAPK. *J. Biol. Chem.* **280:** 31413–31419.
28. Takahashi, Y., W. C. Glasgow, H. Suzuki, Y. Taketani, S. Yamamoto, M. Anton, H. Kuhn, and A. R. Brash. 1993. Investigation of the oxygenation of phospholipids by the porcine leukocyte and human platelet arachidonate 12-lipoxygenases. *Eur. J. Biochem.* **218:** 165–171.
29. Krieg, P., M. Siebert, A. Kinzig, R. Bettenhausen, F. Marks, and G. Fürstenberger. 1999. Murine 12(R)-lipoxygenase: functional expression, genomic structure and chromosomal localization. *FEBS Lett.* **446:** 142–148.
30. Siebert, M., P. Krieg, W. D. Lehmann, F. Marks, and G. Furstenberger. 2001. Enzymic characterization of epidermis-derived 12-lipoxygenase isoenzymes. *Biochem. J.* **355:** 97–104.
31. Flores, A. M., L. Li, N. G. McHugh, and B. J. Aneskievich. 2005. Enzyme association with PPARgamma: evidence of a new role for 15-lipoxygenase type 2. *Chem. Biol. Interact.* **151:** 121–132.
32. Kim, E., J. E. Rundhaug, F. Benavides, P. Yang, R. A. Newman, and S. M. Fischer. 2005. An antitumorigenic role for murine 8S-lipoxygenase in skin carcinogenesis. *Oncogene.* **24:** 1174–1187.
33. Muga, S. J., P. Thuillier, A. Pavone, J. E. Rundhaug, W. E. Boeglin, M. Jisaka, A. R. Brash, and S. M. Fischer. 2000. 8S-lipoxygenase products activate peroxisome proliferator-activated receptor alpha and induce differentiation in murine keratinocytes. *Cell Growth Differ.* **11:** 447–454.
34. Chen, G. G., H. Xu, J. F. Lee, M. Subramaniam, K. L. Leung, S. H. Wang, U. P. Chan, and T. C. Spelsberg. 2003. 15-Hydroxy-eicosatetraenoic acid arrests growth of colorectal cancer cells via a peroxisome proliferator-activated receptor gamma-dependent pathway. *Int. J. Cancer.* **107:** 837–843.
35. Shappell, S. B., R. A. Gupta, S. Manning, R. Whitehead, W. E. Boeglin, C. Schneider, T. Case, J. Price, G. S. Jack, T. M. Wheeler, et al. 2001. 15S-Hydroxyeicosatetraenoic acid activates peroxisome proliferator-activated receptor gamma and inhibits proliferation in PC3 prostate carcinoma cells. *Cancer Res.* **61:** 497–503.
36. Chang, M. S., C. Schneider, R. L. Roberts, S. B. Shappell, F. R. Haselton, W. E. Boeglin, and A. R. Brash. 2005. Detection and subcellular localization of two 15S-lipoxygenases in human cornea. *Invest. Ophthalmol. Vis. Sci.* **46:** 849–856.
37. Wakeman, T. P., D. Wyczechowska, and B. Xu. 2005. Involvement of the p38 MAP kinase in Cr(VI)-induced growth arrest and apoptosis. *Mol. Cell. Biochem.* **279:** 69–73.
38. Peus, D., R. A. Vasa, A. Beyerle, A. Meves, C. Krautmacher, and M. R. Pittelkow. 1999. UVB activates ERK1/2 and p38 signaling pathways via reactive oxygen species in cultured keratinocytes. *J. Invest. Dermatol.* **112:** 751–756.
39. Lapenna, D., G. Ciofani, S. D. Pierdomenico, M. A. Giamberardino, and F. Cuccurullo. 2003. Dihydrolipoic acid inhibits 15-lipoxygenase-dependent lipid peroxidation. *Free Radic. Biol. Med.* **35:** 1203–1209.